NASTRAN Analysis of a Wheel-Rail Loading on Its Foundation

M. S. Katow
DSN Engineering Section

One type of azimuth bearing for a large ground antenna (100 m) will consist of steel wheels, mounted at four corners of the alidade, rolling on a circular flat rail which provides the vertical restraints; a radial constraining bearing at the center of the alidade provides the horizontal restraints. One important design feature is the compressive stresses in the grout or concrete foundation under the wheel-rail load.

This report describes a finite element analysis check of a particular design by H. McGinness that consists of a steel rail resting on a concrete foundation. Symmetry is assumed as much as possible in order to minimize the models, but meaningful element sizes are used. Recently developed isoparametric hexahedron elements available in the NASTRAN computing program, which minimizes the number of elements required while maintaining the accuracy of the computed stresses, are used with two versions of NASTRAN. Test cases to check with the analytical solutions are made. A side loading is also applied to calculate the increase in the concrete stresses.

I. Introduction

One design of an azimuth bearing of a ground antenna restrains the vertical component (mostly the weight) by mounting wheels at the four corners of the alidade, which rolls on a flat surfaced circular rail. The rail, in turn, is supported by a concrete foundation. Figure 1 shows a cross-sectional view of this particular rail-foundation design. The wheel rolls around an approximate 35-m-radius circle on a hardened wear strip fastened to a mild steel rail. This rail is supported by the concrete foundation with a grout material between the two. A one-piece circular rail with welded joints will be required.

II. Model Description

The wear strip and the grout were deleted from the model because of their minimal effects on the design questions at hand.

The first model generated was a two-dimensional type in order to simplify and reduce the model size as much as possible. First, we assumed an infinite number of wheel loads with a 1.02-m separation instead of the actual case of four wheels approximately 1.02 m apart. This enables the use of a model 1/2 of 1.02 m length by using symmetric boundary conditions. If the wheel width is assumed to be infinitely wide along with the concrete foundation, the model is reduced to one element width (0.02 m) of the cubic hexahedron elements.

Thus the computer model shown in Fig. 2 has uniform stresses across the width of the rail/foundation. The smallest element size of 0.02 m cube occurs for the concrete just under the wheel loads on the steel rail where the stress is the highest. The long aspect ratio elements are farthest from the concentrated loading.

The steel rail in Fig. 2 is modeled by the linear isoparametric hexahedron cubes with six layers in depth. Connections are made between the bottom modes of the rail and the top modes of the concrete foundation with MPC (multipoint constraint) sets, which transfer only vertical or Z forces. This simulates the two surfaces in sliding connection, transferring vertical forces only.

In Fig. 3, the steel rail is modeled by NASTRAN's CBAR beam elements, which requires inputs of the cross-sectional area, moment of inertia, Young's and shear moduli, and the shear area factors. Two rows of CBARS are required to replace the one layer of hexahedron modeled beam.

In order to first test the accuracy of the steel rail models, they were modeled separately and NASTRAN-analyzed. Figure 4 shows the modeling techniques. In effect, the continuous concrete reaction points were replaced by one reaction at the center, thus reducing the model to a center-loaded beam with fixed ends. In other words, the model is equivalent to four cantilever beams of length 0.255 m, each connected at the inflection points M.

The cantilever beam with a built-in cross section (Fig. 4-III) that is completely prevented from warping has an analytical solution (Ref. 3). The $-Z/2$ deflection δ equals

$$\delta = \frac{Pl^3}{3EI}\left(1 + 0.74\frac{h^2}{l^2} - 0.01\frac{h}{l}\right)$$

The terms in the parenthesis cover the shear deflection for a rectangular cross section beam where

l = length (0.255 m)

P = load

h = depth of cross section

E = Young's modulus

I = moment of inertia

$$E' = E\left(\frac{1}{1 - \mu^2}\right)$$

μ = Poisson's ratio = 0.3 for steel

The initial models (sequence number 3 to 5 in Table 2) used the meshes shown in Figs. 2 and 7 where the finer divisions are in the left end. Because this mesh can be improved for concentrated loadings at both ends, Fig. 5 shows the symmetric divisions used for models of sequence numbers 7 and 8 of Table 1.

The loading applied to the beam-rail and the two-dimensional models was computed by assuming that the wheel width was equal to the rail width of 0.61 m. Then the loading at the corners of the 0.02-m-wide models equals

$$2{,}624{,}550\ N(590{,}000\ \text{lb}) \times \frac{0.02}{0.61} \times \frac{1}{4} = 21{,}526\ N$$

Figure 6 shows how the loading for the three-dimensional model (Fig. 7) was derived.

Finally, a three-dimensional model was generated as shown in Fig. 5. The 0.04-m smallest cube was used for this model since computing costs were a factor for models of this large size. A sup time of one hour was required on the 1108 computer.

III. Analysis Discussion

The isoparametric solid hexahedron element appeared in level 16 of NASA NASTRAN (Ref. 1). MSC NASTRAN (Ref. 2) had an earlier version of this element which was recently modified to improve the deflection computation due to shear stresses. The stresses and deflections can vary through each element so its use allows a more accurately defined structure with fewer elements. These elements take into account pressure loads, which are of primary interest in the problem under discussion.

With no previous experiences in the use of these elements, a decision was made to utilize both versions of NASTRAN, since it appeared that the finally developed elements were independently generated. This analysis method should provide some checks on the veracity of our inputs and computed outputs.

To minimize the input data errors, a 1108 program was written to generate the complete input data for the three-dimensional problem shown in Fig. 7. It was only necessary to define the number of elements in the three directions and the progressive element lengths. The two-dimensional models were generated by editing out extraneous data and adding constraints where necessary. By progressively increasing the GRID numbers for the foundation portion through each cross-section to the next cross-section and adding a large number to the connecting GRID nodes to the top steel beam and repeating the numbering operation for the beam itself, the NASTRAN runs were made with minimum spillage and acceptable run times.

The cantilever beam deflection equation (Eq. 1) was derived (Ref. 3) for application to the usual finite cross-sectional beams. By replacing E with the flexural rigidity quantity E' or $E(1/1 - \mu^2)$, the equation is applicable to the segment of an infinitely wide beam, as used in Table 1 (Ref. 4).

The important compressive stress to be resolved is in the concrete foundation directly under the wheel loading point. The concentrated loadings on the rail must be dispersed as the effect of the loading progresses through the thickness of the rail to the bottom contact to the concrete. The thickness as well as the width should be important to the degree that the vertical loads are dispersed, while the width will be a factor for the side loading from the wheel.

The accuracy of this computed compressive stress will be highly dependent on accurate modeling of the steel beam-rail. For this determination, the beam alone was modeled as shown in Fig. 4. Since the hexahedron model accepts pressure loads and localized deflections occur, the total deflection number is also given for this model (Fig. 4-I) as well as the deflection of the neutral or center axis of the beam.

The localized deflections from these pressure loads on the bottom of the steel beam seem to have a large effect on the generated compressive stresses in the concrete. Figure 8 delineates the pressure forces in the MPC connections between the beam and the concrete nodes for the two-dimensional models as output by the GRID-point-force balance table.

IV. Results

Comparison of the $-Z$ deflections between the analytical cantilever beam (Fig. 4-III) and the CBAR beam (Fig. 4-II) shows a close match. The observation can be made that the CBAR element of NASTRAN accurately computes the shear deflections. The shear deflection is almost half of the bending in this model.

If the center axis (neutral axis) $-Z$ deflections of the NASA hexahedron beam is compared to the cantilever beam deflection, it is stiffer by about 15 percent. If the localized deformations from the concentrated loading are accounted for by comparing the $-Z'$ deflections, the standard beam is slightly stiffer (Table 1).

The two-dimensional beam and concrete models described in Table 2 show much higher node 2001 (Figs. 2 and 3) compressive stresses for the CBAR beam model: higher than explainable by the almost equal bending stiffnesses shown in Table 1 data. The slightly higher bending stiffness of the hexahedron may account for part of the decrease in compressive stresses. However, the localized deflections from the pressure loads must be responsible for a large portion of the differences of the compressive stresses. In Fig. 8, the pressure forces between the beam-rail and the concrete show large differences between the models.

From the foregoing data, it is recommended that the results from the hexahedron models using the 0.02 m smallest cubic elements should be increased 10 percent to account for their stiffer bending/localized deformation characteristics. The tolerance on this percentage is approximately plus 5 and minus 10. More analysis checks on the accuracy of the hexahedron models should be done.

Also, another 5 percent should be added for the increase in the smallest element size from 0.02 m to 0.04 m. Here again, more use experiences would be helpful in optimizing computer run time against accuracies in the computed results.

Bibliography

1. "The NASTRAN User's Manual," Level 16.1, National Aeronautics and Space Administration.
2. "The NASTRAN User's Manual," MSC-41, McNeal-Schwindler Corp., Los Angeles, Calif.
3. Timoshenko, S., "Strength of Materials," Part I, *Advanced Theory and Problems,* D. Van Nostrand Co., Inc., 1930, p. 191.
4. Timoshenko, S., "Strength of Materials," Part II, *Advanced Theory and Problems,* D. Van Nostrand Co., Inc., 1930, p. 475.

Table 1. Steel beam-rail only, vertical deflections

Seq	Beam type	NASTRAN level	$-Z$ deflection $\times 10^4$[a] m with E	with E′	$-Z' \times 10^4$[b] m with E	Remarks	Program
1	Cantilever (Eq. 1)	--	-2.47	-2.28[c]	--	Fig. 4-III	--
2	CBAR	NASA-16.1	-2.45	-2.23	--	Fig. 4-II	F1CTNAST
3	Hexahedron	NASA-16.1	-1.98	--	-2.35	0.02 mesh, Fig. 5-I	F1CUNAST
4	Hexahedron	MSC-41	-2.11	--	-2.51	0.02 mesh, Fig. 5-I	FGANAST
5	Hexahedron	NASA-16.1	-1.69	--	-1.98	0.04 mesh, Fig. 5-II	F7BNAST
6	Hexahedron	MSC-41	-1.96	--	-2.24	0.04 mesh, Fig. 5-II	F7ANAST
7	Hexahedron	NASA-16.1	-2.10	--	-2.68	0.02 mesh, Fig. 5-III symmetric	F1ONAST
8	Hexahedron	NASA-16.1	-2.02	--	-2.47	0.04 mesh, Fig. 5-IV symmetric	F9NAST

[a]$-Z$ Deflections are the neutral axis $-Z$ differentials. E = Young's modulus, 2.1×10^{11} n/m^2, $E' = E(1/1 - \mu^2)$ μ = Poisson's ratio, 0.3.

[b]$-Z'$ deflections measured per Fig. 4-I (includes compressive deformations from concentrated loads).

[c]E′ used for the bending deflection portion.

Table 2. Concrete compressive stresses (node 2001), two-dimensional models (Figs. 2 and 3)

Seq	Steel rail-beam	NASTRAN level	Concrete stresses, $\times 10^{-6}$ N/m^2 ($\times 10^{-3}$ psi) Node 2001 compressive	Element mean pressure	Element octahedral shear	Remarks	Run no.
1	CBAR	NASA-16.1	-11.55 (-1.68)	7.03	3.88	Used E′, Fig. 3	FIBNAST
2	CBAR	MSC-41	-11.44 (-1.70)	6.97	3.60	Used E′ Fig. 3	FIBNAST
3	Hexahedron	NASA-16.1	-7.08 (-1.03)	4.63	2.47	Mesh = Fig. 5-I	FICNAST
4	Hexahedron	MSC-41	-7.86 (-1.14)	4.66	2.48	Mesh = Fig. 5-I	FICNAST
5	Hexahedron	NASA-16.1	-7.53 (-1.09)	4.39	2.43	Mesh = Fig. 5-II	F7ANAST

Table 3. Concrete compressive stresses/three-dimensional model (Fig. 7)

Seq	NASTRAN level	Loading	Top of concrete – compressive stress, × 10^{-6} N/m^2 (× 10^{-3} psi)[a]						
			*A	B	C	D	E	F	G
1	NASA 16.1	Top 2,624,450 N	−10.22	− 9.94	−9.00	−8.08	−6.88	−5.54	−5.17
2	NASA 16.1	Side 868,000 N	0.0	± 0.70	±0.77	±0.91	±1.04	±1.27	±2.39
3	NASA 16.1	Total (max)	−10.22 (1.48)	−10.14	−9.77	−9.00	−7.92	−6.81	−7.56
4	MSC-41	Top 2,624,450 N	−10.39	−10.11	−9.35	−8.27	−7.10	−5.77	−5.61

[a]A – G = locations designated on Fig. 7

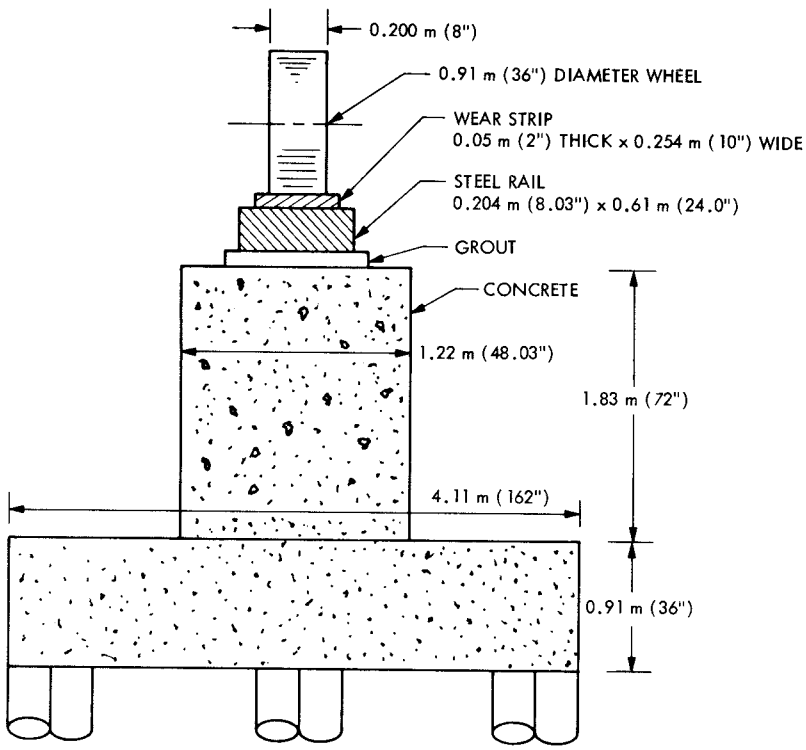

Fig. 1. Cross-sectional view, rail-foundation

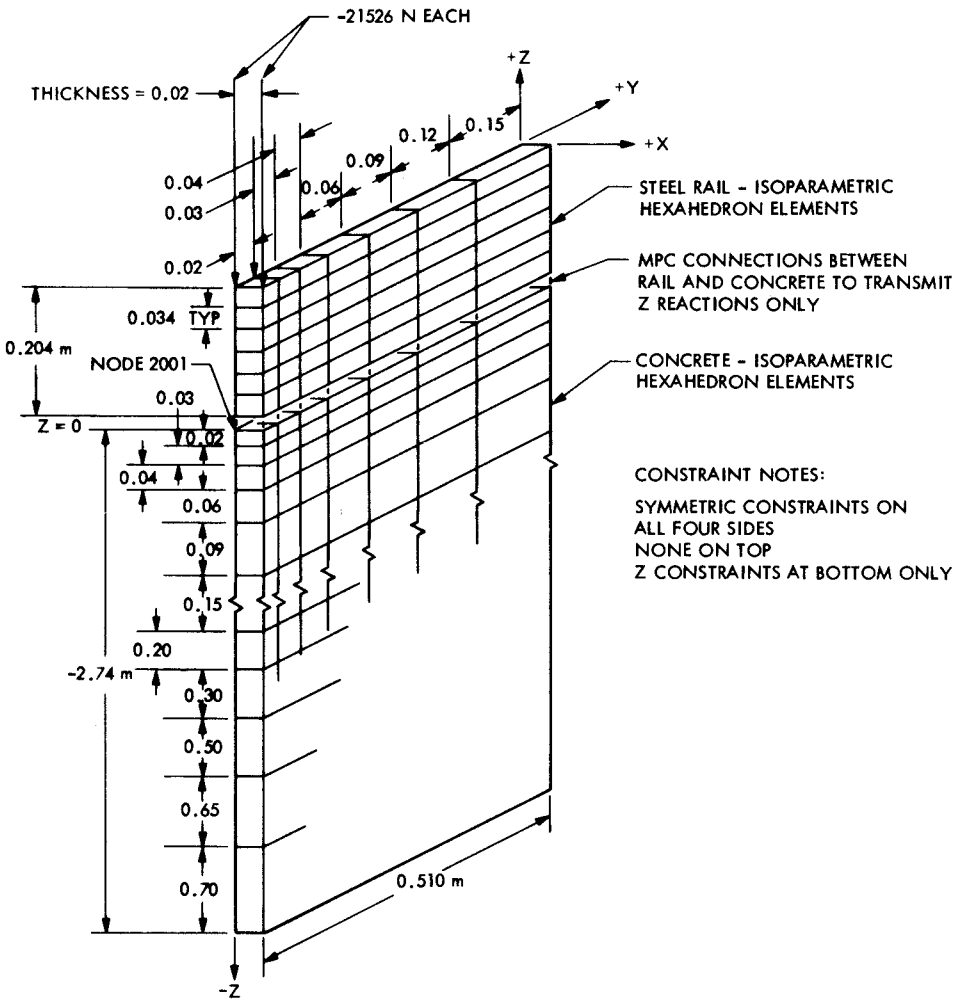

Fig. 2. Two-dimensional hexahedron model

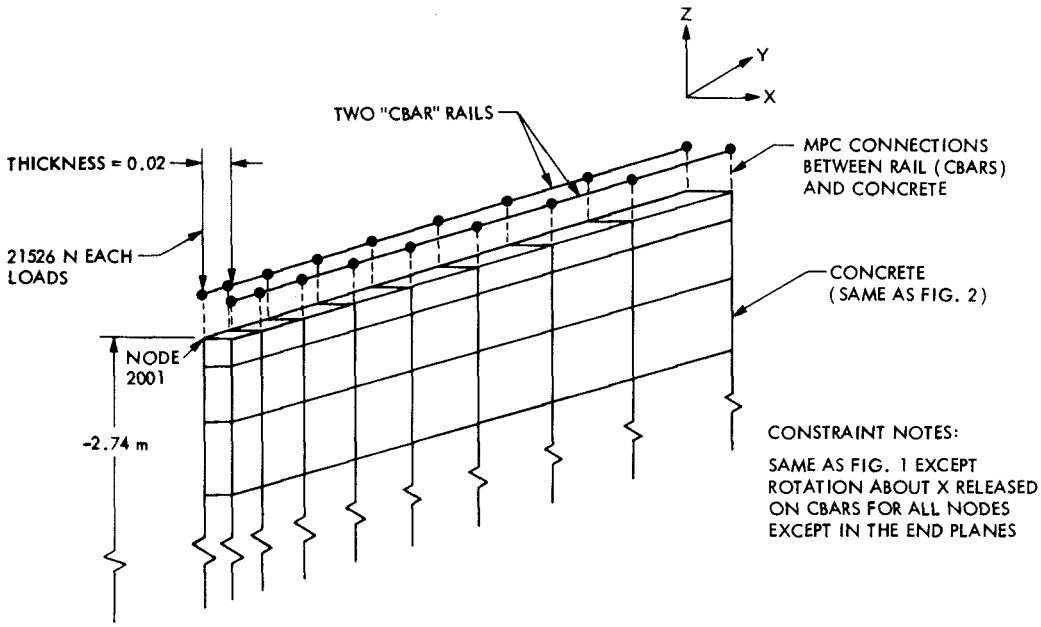

Fig. 3. Two-dimensional CBAR-hexahedron model

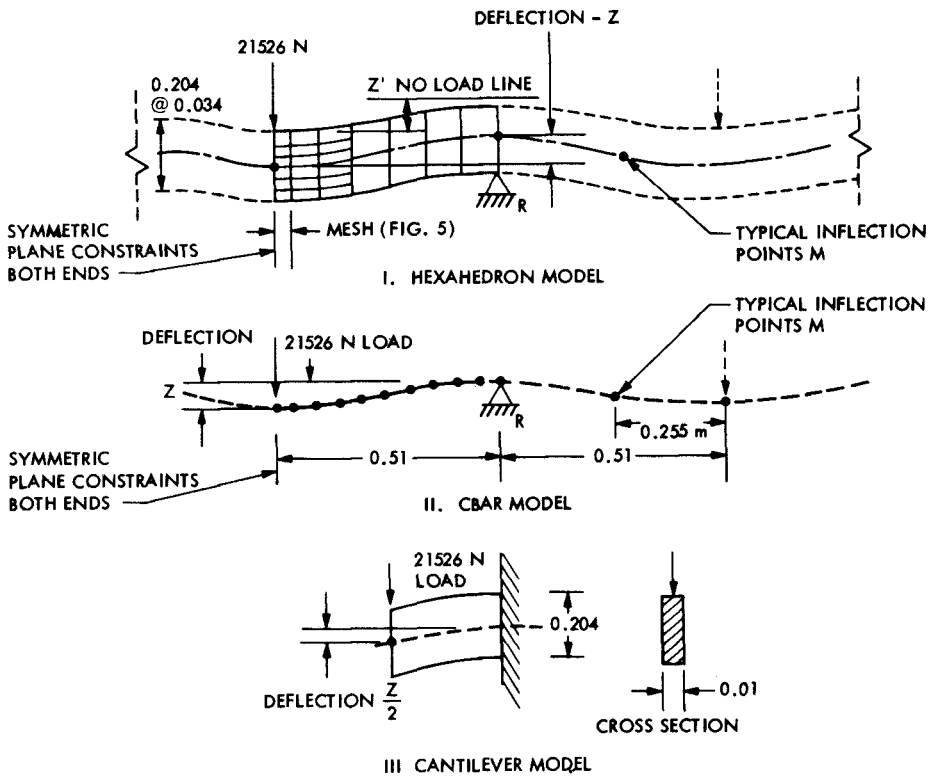

Fig. 4. Steel beam-rail only models

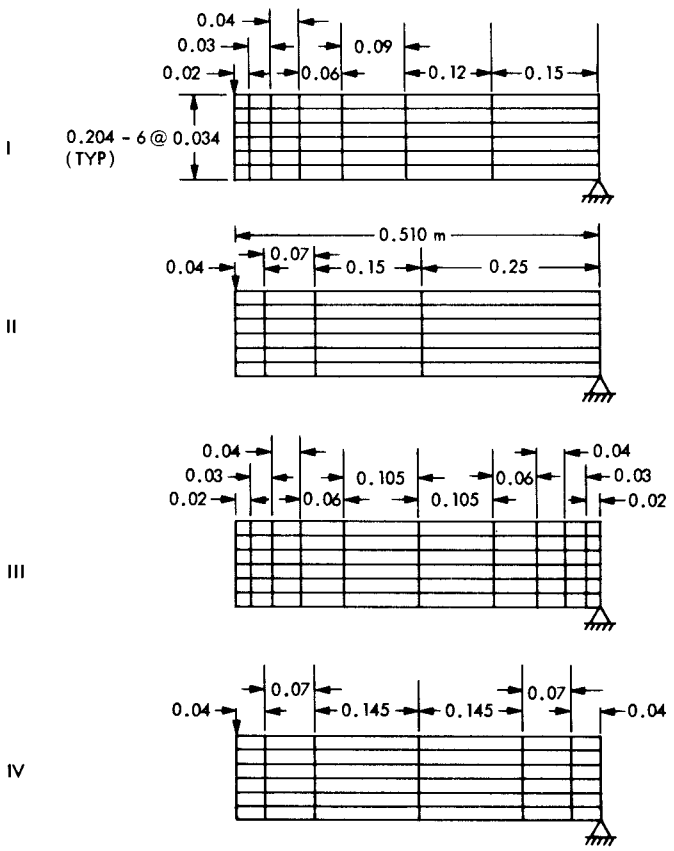

Fig. 5. Two-dimensional model, meshes

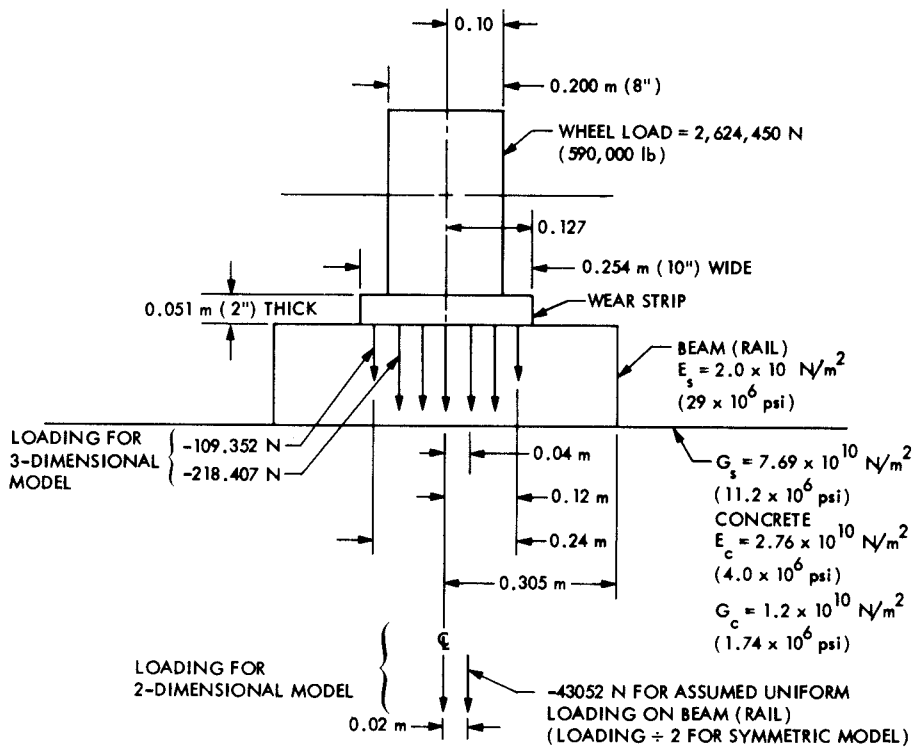

Fig. 6. Wheel loading data

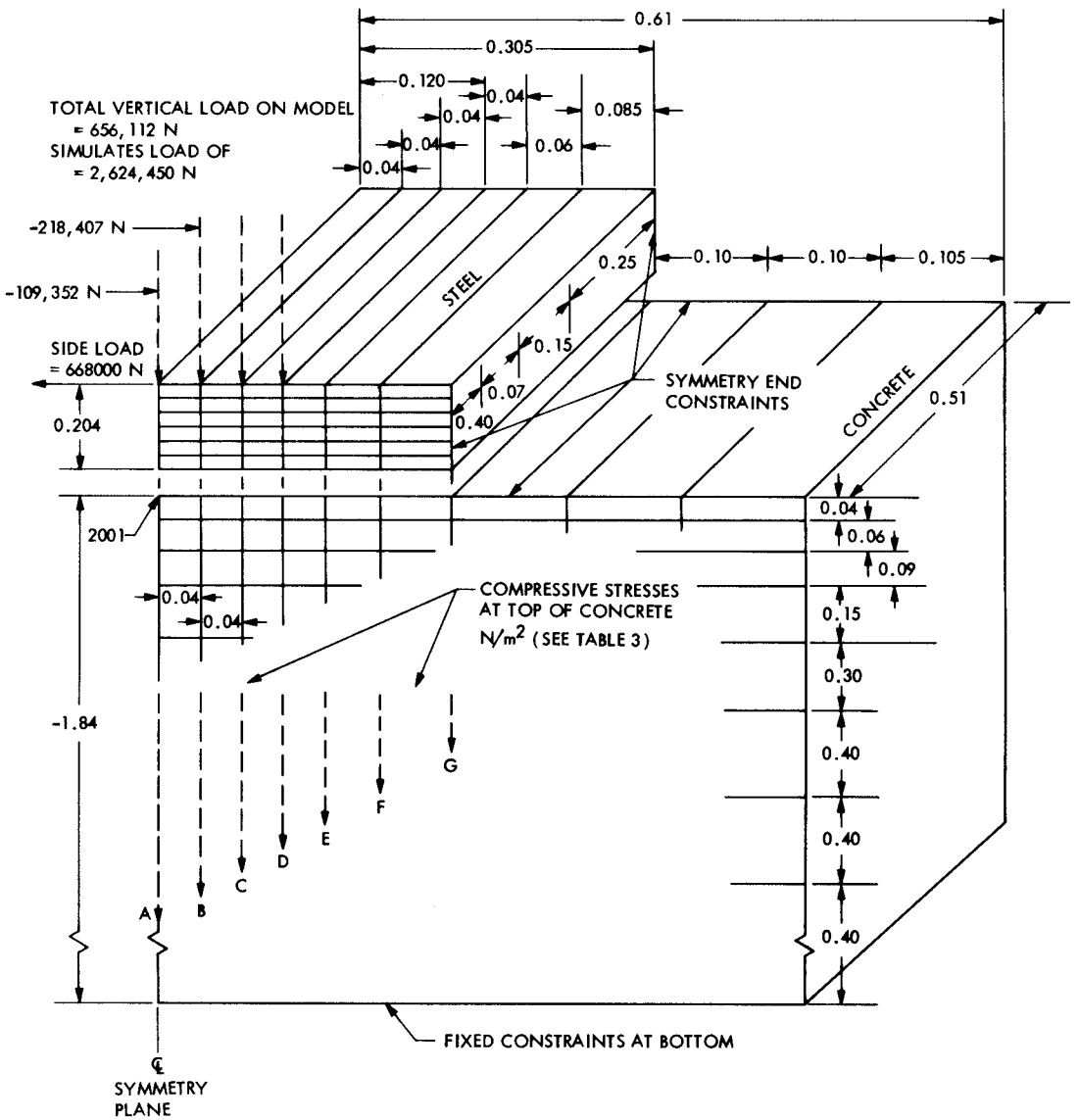

Fig. 7. Three-dimensional model

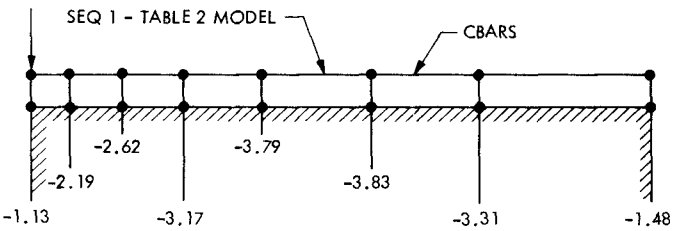

I. CBAR MODEL, FIG. 3

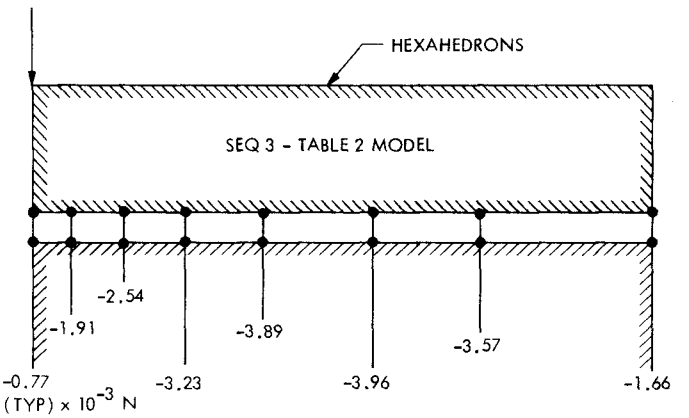

II. HEXAHEDRON MODEL, FIG. 2

Fig. 8. Pressure forces between beam-rail and concrete